Draft version June 21, 2022

Classifying and Applying Bolometric Corrections to KSP-ZN7090

Patrick Sandoval[1] and Dae-Sik Moon[1,2]

[1] *University of Toronto*
[2] *Department of Astronomy*

1. INTRODUCTION

In this short report we discuss the progress made on our study for KSP-ZN7090 a supernovae with remarkable early data taken by the KMTNet less than one day after the explosion. The observation taken by the Korean Microlensing Telescope Network (KMTNet) are in the B, V, and i bands and they are particularly rare and of high value, note that the the last band is calibrated with respect to the Sloan filter (i). The bolometric corrections used in this paper are with respect to a combination of Johnson Cousin filters with Sloan and a solely Johnson (B - V). In this report we present the criterion's used to classify our supernovae solely based on the V-band light curve morphology in accordance with the parameters set by Anderson et al. 2014 and Gall, E. E. E. et al. 2015. Having classified ZN7090 we proceed to apply various bolometric correction from Martinez et al. 2022, Lyman, Bersier, and James 2013 and Lyman, Bersier, James, Mazzali, et al. 2016a in order to construct the bolometric light curve of our supernovae. It is important to note that we are not generating our bolometric light curve through the direct integration of the SED as we only have data in three bands which will render insufficient for an integration in all the wavelengths.

1.1. *Classification of Supernovae Based on Light Curve Morphology*

Historically SNe have been broken down into two groups based on their spectral information, Type I lack hydrogen emission line in their spectrum while Type II SNe have strong hydrogen emission lines. Withing the Type II classification there exists two subdivisions based solely on the morphology of the V-band light curve, Type II-L and Type II-P. The former has linear decline post peak magnitude while the latter has plateau phase post peak hence the L and P in their classifications. In Anderson et al. 2014 and Gall, E. E. E. et al. 2015 they study a large samples of Type II-L and Type II-P in order to quantify the defining characteristics of each light curve. The key take-away from these studies is that Type II-L SNe have a post peak decline rates greater than a hundredth of a magnitude per day.

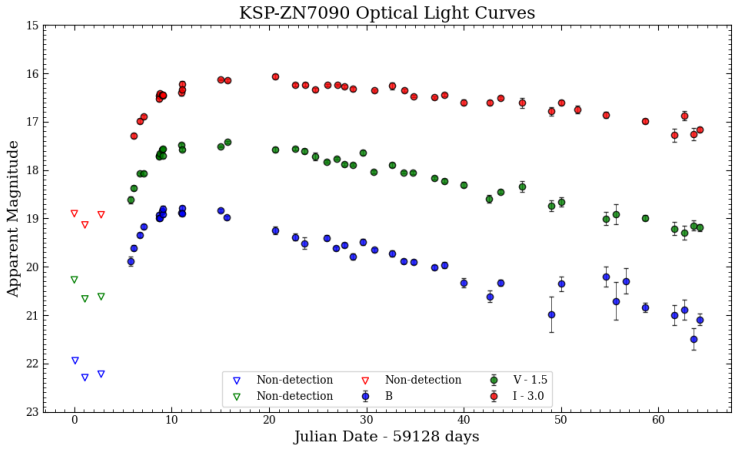

Figure 1: KSP-ZN7090 B, V, and I light curves, after applying color corrections, extinction corrections and binning. V and I light curves have been vertically displaced by equal amounts for easier comparison. All light curve data was collected from `ZN7090_LC_20220309_correct.csv`, from the `M_E` column. While the non-detection data points were collected from the `M_E_lim` column

From Figure 1 we see a strong linear trend post peak for the V-band light curve, however, it is not entirely clear where V-band peaks and therefore the epoch of m_{max} is not easily constrained. In the following section we address this problem and constrain the peak magnitude epoch and compute the magnitude decline post peak.

2. DATA REDUCTION & METHODS

2.1. *High Order Polynomial Fitting on Light Curves*

High order polynomial fits have been used in literature before to estimate the peak epoch Shappee et al. 2018, in this case the most common polynomial used for light curve fitting is a polynomial of degree six or seven. For this fitting we performed a Monte-Carlo Gaussian sampling on each data point of the light curve. Then we on every set of sampled point in the light curve we fitted a polynomial of degree 7. This method randomly sampled 100 points on each data and averaged the coefficients of the individual fits to create the average polynomial curve as seen in Figure 2. With this model fit we can improve our estimates of the peak epoch and can compute the decline rate of the V-band light curve. This fit was also performed on the other two light curves as the peak epoch is a very important parameter which we will discuss on later on this paper. With the peak epoch properly constrained we can fit a polynomial of

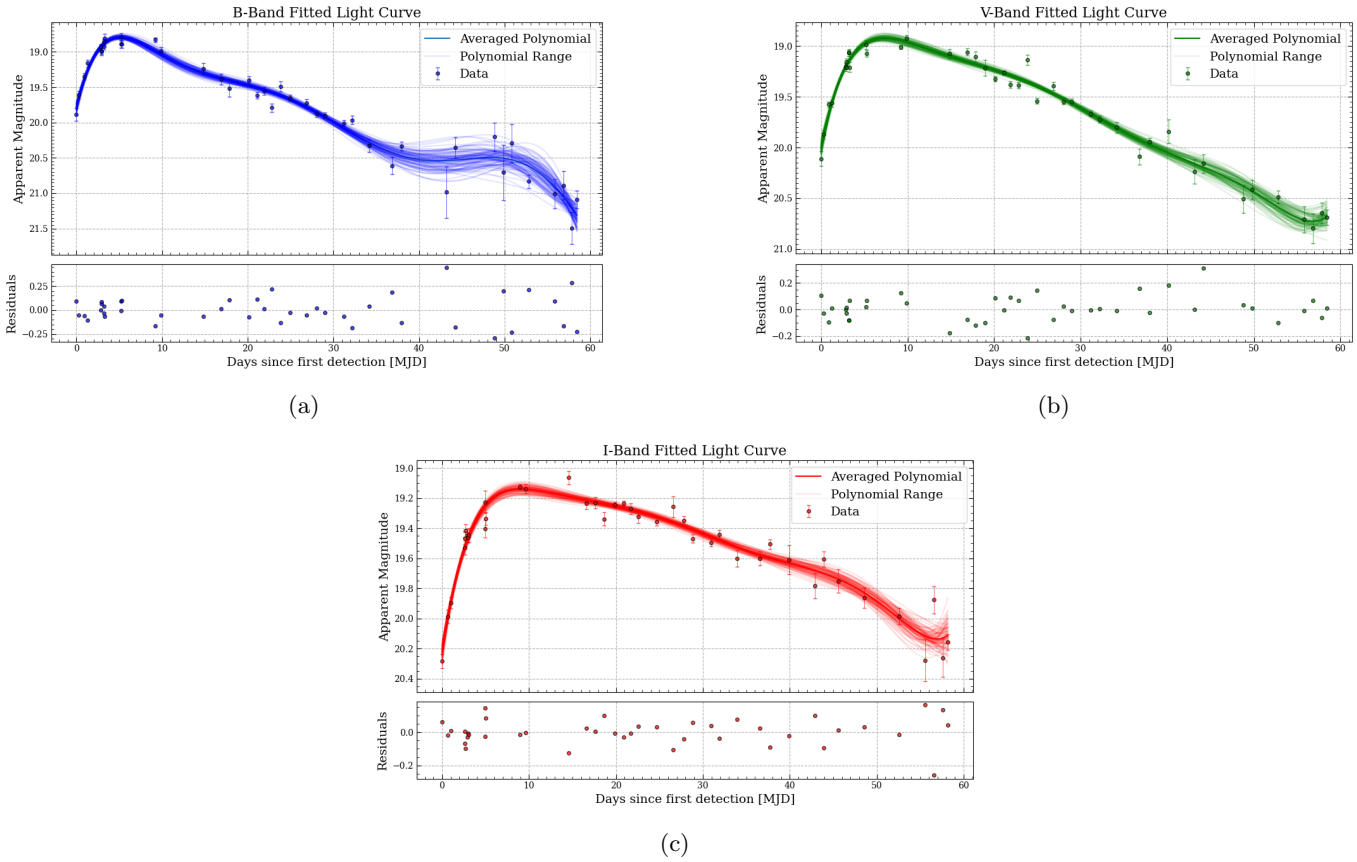

Figure 2: High order polynomial fitting on optical light curves of KSP-ZN7090, done through Monte Carlo Gaussian sampling of individual data points. (Solid dark lines) are the polynomials with the averaged coefficients from all the Monte Carlo simulation, and the (solid transparent lines) are the individual computed polynomials from each sampling. The peak epochs are 5.1 ± 0.2, 7.3 ± 0.3 and 9.0 ± 0.3 for the B, V and I light curves respectively. Note that all the dates are standardized with respect to the date of the first detection in that band.

degree one past this epoch and compute the decline rate of the V-band light curve to be 3.84 ± 0.01 mags/100 days. We clearly see that the decline of the V-band light curve satisfies the condition specified in 1.1. This provides strong evidence that ZN-7090 is a Type II-L SNe instead of a Type II-P.

2.2. *Interpolation Methods for Light Curves*

In order to apply the bolometric corrections from Martinez et al. 2022, Lyman, Bersier, and James 2013 and Lyman, Bersier, James, Mazzali, et al. 2016a we need our magnitudes in the B,V and i bands to be in the same epoch, if we carefully study Figure 1 we see that some points in certain magnitudes do not have corresponding data in the other magnitudes. In order to address this issue we tried several different interpolation methods and opted to perform spline linear interpolation on the light curves as this method preserved the shape of the light curve. However, there is one early data point in the I-band that we cannot interpolate, and that is the corresponding first detection data point for the B,V bands, which occurred on October 12, 2020 at 14:44 while the first recorded detection of the I-band was on October 12, 2020 at 14:47, this means we will need to extrapolate roughly 3 hours back in time for the first detection of the I-band to match the first detection of the B and V bands.

2.3. *Extrapolation of I-band*

In order to extrapolate the I-band light curve 3 hours back in time we will be using a variety of different analytical function and we will compare the results of the extrapolation and pick the method we believe to be more representative of the early stages of the light curve. We will be using a polynomial of degree 7 as implemented in section 2.1, we will be using a power law as shown in section 1, where we constrain t_0 to be the result obtained through the simultaneous fitting implemented in section 3.2.1. We notice that the spline linear interpolation falls in between the polynomial fit

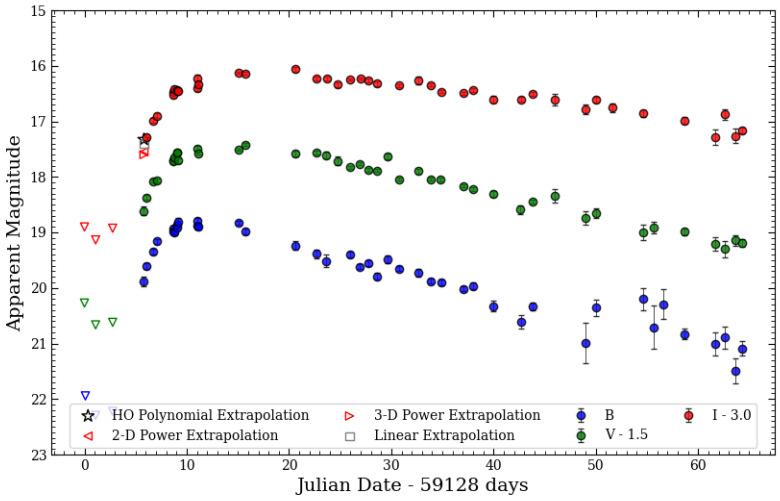

Figure 3: Extrapolation of I-band light curve 3 hours prior to first detection. Extrapolated magnitudes for each model are; High order polynomial (20.32), 2 day power law (20.55), 3 day power law (20.60) and linear (20.41)

and the power fit, however, when it comes to physical motivation as to which model would be more suitable for an extrapolation then we suggest using the 2 day power model as this model has the correct assumption of zero flux at first light and does not lead divergences like high order polynomials do when extrapolated outside the data domain.

3. DATA ANALYSIS & MODELING

With the light curves interpolated and with all the data points having matching dates we can begin to apply the bolometric corrections from external literature in order to construct the bolometric light curves. It is important to note that the KMTNet's (B) and (V) are calibrated with respect to Johnson Cousin filters while (i) is calibrated with respect to the Sloan filter, therefore, the correction we must apply must be compatible with these filters.

3.1. *Martinez Cooling Bolometric Correction*

The bolometric corrections provided by this paper are split into 3 different sections corresponding to the different phases of a Type II-P SNe, shock cooling, plateau and radioactive/nebular phase. As discussed in 2.1 we do not believe ZN-7090 to be a Type II-P SNe therefore we will not use the corrections for that phase. Additionally, we will not

use the radioactive tail correction because we have do not observe such behaviour in early epoch of the light curve Anderson et al. 2014 usually such behaviour is seen at a epoch > 100 days from the explosion. Therefore, the only correction that we will be using from this paper is for the shock cooling phase.

Table 1: Martinez et al. 2022 bolometric correction coefficients for polynomial of degree 4 specific to the shock cooling phase.

Color	Phase	Range	c_0	c_1	c_2	c_3	c_4	σ
B - V	Cooling	(-0.10,1.16)	-0.740	4.472	-9.637	9.075	-3.290	0.12

NOTE—BC $= \sum_{k=0}^{n} c_k \, (color)^k$ where color is taken from column 1. σ is the standard deviation about the fit.

3.1.1. *Monte-Carlo Gaussian Sampling*

In order to apply the correction specified by this paper we need to first compute the colors for this correction, colors are often referred to as the difference between two magnitudes, in the case of this paper we are only provided a single color (B - V). So for the uncertainty propagation for this correction we implemented a Monte Carlo Gaussian sampling method where we sample data points from our light curves and compute the color, bolometric correction terms and the bolometric magnitude.

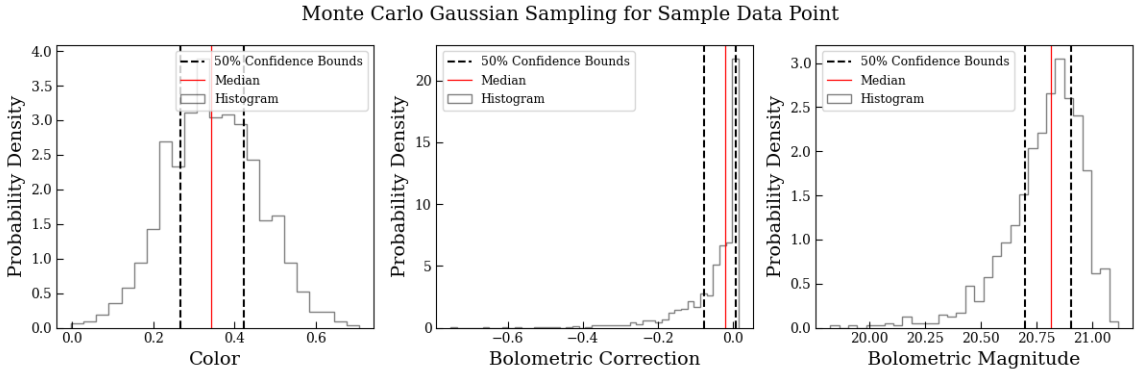

Figure 4: Probability distributions for Gaussian sampling method on bolometric corrections.(Dashed lines) indicates the boundaries of the 50% confidence interval, (Solid red line) indicates the median of the distribution.

The most important aspect to take away from Figure 4 is that the bolometric magnitude distribution is asymmetric, which means a good measure of the spread of the distribution is the interquartile range instead of the standard deviation, as this quantity provides us information regarding the asymmetry of the distribution. Additionally, because our distribution is asymmetric we are using the median instead of the mean because the median is as better statistical representation about the populations true distribution.

3.1.2. *Bolometric Correction & Color Sensitivity*

After applying the Gaussian sampling method outlined in section 3.1.1 we can now take a look the the bolometric light curve and also look at several other plots which provide us with insightful information about the nature of the correction itself.

From Figure 5 we can see that much of the early data that we have on ZN-7090 is not within the range of colors specified by the correction, however, this is to be expected because early data on SNe is very rare therefore these negative colors are rather uncommon to see in literature. We see this play a noticeable role in our bolometric light curve as we can see on the top left panel there are two data points with error bars of around 3 magnitude which rises concern about the origin of those two points. We can then note the bottom right figure and locate these same two points outside the effective range, from this observation we can notice that all color data points outside the effective

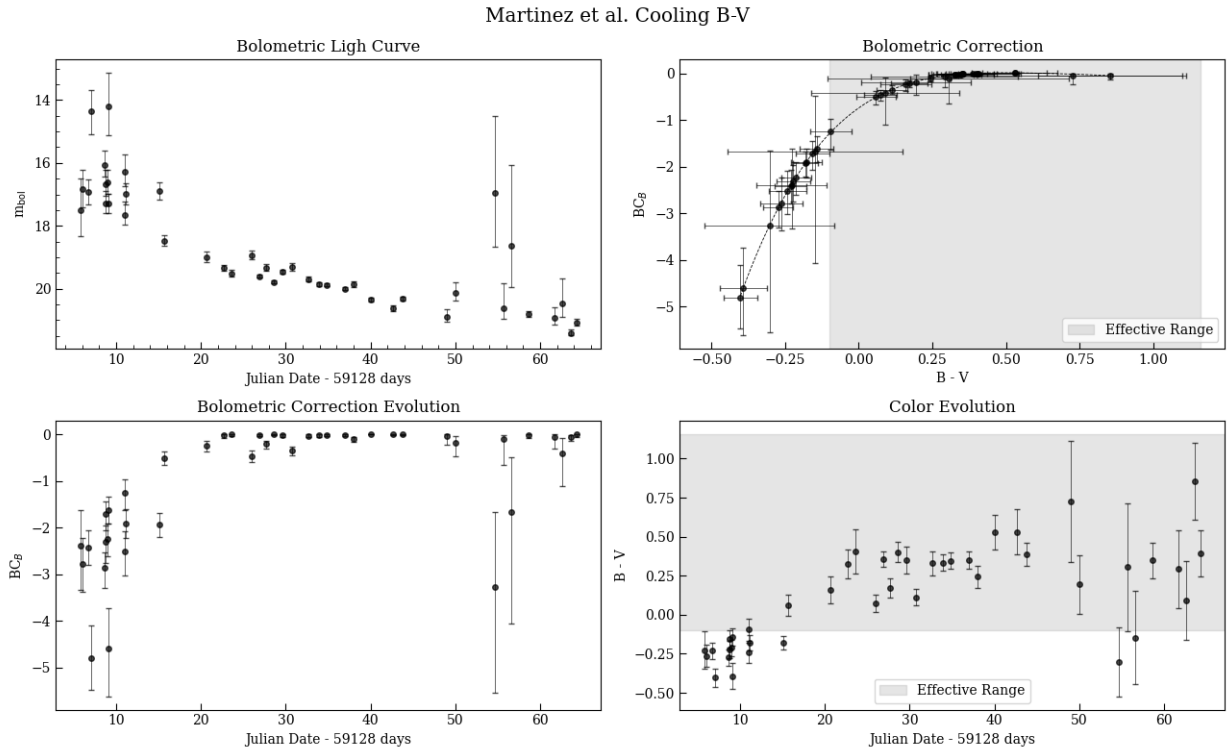

Figure 5: (Top left panel) Bolometric light curve where data points are the median of the Monte Carlo Gaussian sampling distribution and error-bars are the IQR of the sampling.(Top right panel) Bolometric correction as a function of color, shaded region is the color range from the SNe sample used in Martinez et al. 2022. (Bottom left) Bolometric correction term evolution through time, (Bottom right) Color evolution through time.

range have their bolometric correction term uncertainty increase. We can probe the sensitivity of the correction to color by slightly changing/perturbing the color and measuring the respective change in bolometric correction. Then the ratio between the change in bolometric correction to the change in color will tell us how sensitive the correction is to color.

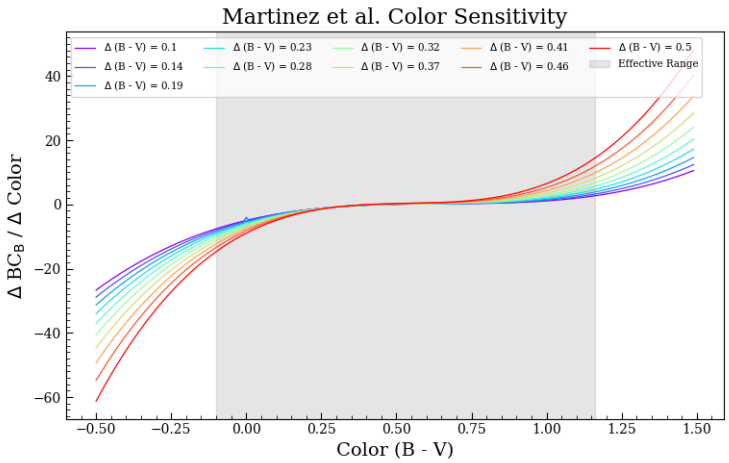

Figure 6: Color sensitivity plot for Martinez et al. 2022 bolometric correction where y-axis measures the change in the correction compared to the change in color. Different colored lines have different color perturbations in percentages as indicated in the legend.

From Figure 6 we see that higher perturbations in the color lead to even higher changes in the bolometric correction when we are outside the range provided by the paper. This tells us that the bolometric correction is highly sensitive to colors specially the ones located outside the effective range.

3.2. *Layman Cooling Bolometric Corrections - 2014*

As opposed to the correction presented in section 3.1 Lyman, Bersier, and James 2013 offers a wider variety of bolometric corrections for a wider range of color (B - V), (B - I), and (V - I) for the Johnson cousin filters, however, we must note that we cannot use the the latter two because our I-band is calibrated with respect to the Sloan filter, and the conversion from Sloan to Johnson is yet to be established. Additionally, the corrections are split up into two phases, cooling and radiatively-/recombination-powered phases. Therefore, in order to apply these correction we need be able to determine the powering mechanism that is driving the light curve. The observable difference between these two powering mechanism is the light curve's rise time from first light to peak magnitude González-Gaitán et al. 2015.

3.2.1. *Constraining First Light*

As previously shown in section 2.1 we have been able to constrain the peak epoch for all three light curves, now we need to find the epoch of first light. For this we need to fit a power law to our data points prior to the first detection and up to the half of the peak magnitude González-Gaitán et al. 2015. However, if we were to follow this criteria for our fitting we would only be able to fit two data points to eq.1 for each light curve. The reason why González-Gaitán et al. 2015 recommends to use up to the half the peak magnitude dates is to avoid over-estimating the first light epoch since the peak magnitude date is highly sensitive to the cadence of observations. In order to obtain a reliable fit and avoid over-estimates we will be creating two scenarios for our fit, one were we fit the data up to 2 days since the first detection and one where we fit the data up to 3 days since the first detection.

$$f = \begin{cases} a(t - t_0)^n & t \geq t_0 \\ 0 & t < t_0 \end{cases} \tag{1}$$

With this method we compute the rise time of each scenario, our results from this computation are shown in the table below.

Table 2: Light curve rise times for power fits in different scenarios

KMTNet Band	2 Day Model (Days)	3 Day Model (Days)
B-Band	5.4 ±0.3	5.5 ±0.3
V-Band	7.5 ±0.3	7.6 ±0.3
I-Band	9.5 ±0.3	9.6 ±0.3

NOTE—The fits were performed simultaneously for each model, meaning that all three power fits have the same t_0, because if the powering mechanism is either from shock cooling or radioactive decay the first electromagnetic emission happens at nearly the same time for all wavelengths.

As we can see, rise times vary depending on the wavelength observed, in column 4 of table 3 from González-Gaitán et al. 2015 we can see the rise time of SNe believed to be powered by shock cooling. We see that B-band shock cooling light curves have median rise time of $6.1^{+2.5}_{-2.3}$, $7.9^{+3.6}_{-2.9}$ for V-band and $10.1^{+3.6}_{-2.3}$ for I band. Meanwhile in Lyman, Bersier, James, Mazzali, et al. 2016b their study in SE SNe, which are believed to be powered by radioactive decay of ^{56}Ni and ^{56}Co, have an average V-band rise time of 17.6 days. This is a strong suggestion that ZN-7090's light curve is primarily powered by shock cooling emission rather than the decay of ^{56}Ni.

3.2.2. *Bolometric Corrections*

Now that we have been able to constrain the powering mechanism for the light curve we can starts applying the bolometric correction from Lyman, Bersier, and James 2013 that are specific to shock cooling. Additionally, after 2 years of this publication the same three authors publish a paper on their study of a sample of SE SNe, where they have 9 Type II-b SNe. In this paper Lyman, Bersier, James, Mazzali, et al. 2016a they provide bolometric corrections for SE SNe and for Type II SNe, however, unlike their previous paper its not clear what mechanism is powering these Type II SNe. Although, in section 2.2 of this paper they comment that their analytical models assume SE SNe are powered by radioactive decay of ^{56}Ni and ^{56}Co this is not necessarily the case for Type II-b SNe as stated in Rubin et al. 2016

Table 3: Lyman, Bersier, James, Mazzali, et al. 2016b bolometric correction coefficients for polynomial of degree 2 specific to the shock cooling phase.

Color	Phase	Range	c_0	c_1	c_2	σ
B - V	Cooling	(-0.2,0.5)	-0.393	0.786	-2.124	0.089
B - i	–	(-0.392, 2.273)	-0.155	-0.450	-0.167	0.023
V - i	–	(-0.391, 0.658)	0.181	-0.212	-1.137	0.044

From table 3 we can see the wider range of colors for the bolometric corrections of the 2016 paper, which altogether makes these two correction more favorable as this indicates that there will not be too much extrapolation outside the color range.

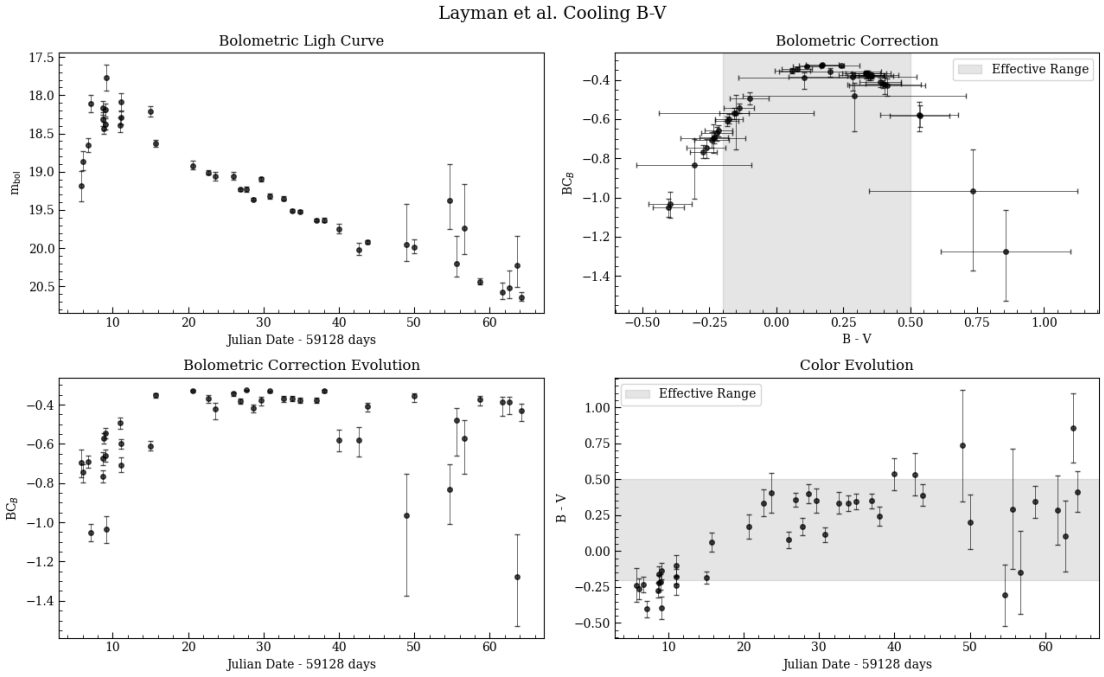

Figure 7: Bolometric corrections from Lyman, Bersier, and James 2013 for (B - V) color as shown in table 3 1^{st} row.

We see throughout Figures 7 - 9 that the color evolution follows a near monotonic behaviour which depicts the transition of the SNe from bluer to redder colors, this is also an indication of the temperature of the SNe, which can be modeled as a smooth function. We can use this idea in order to smooth the color evolution curve through a Monte-Carlo high order polynomial fitting similar to the one presented in section 2.1. By performing a Monte-

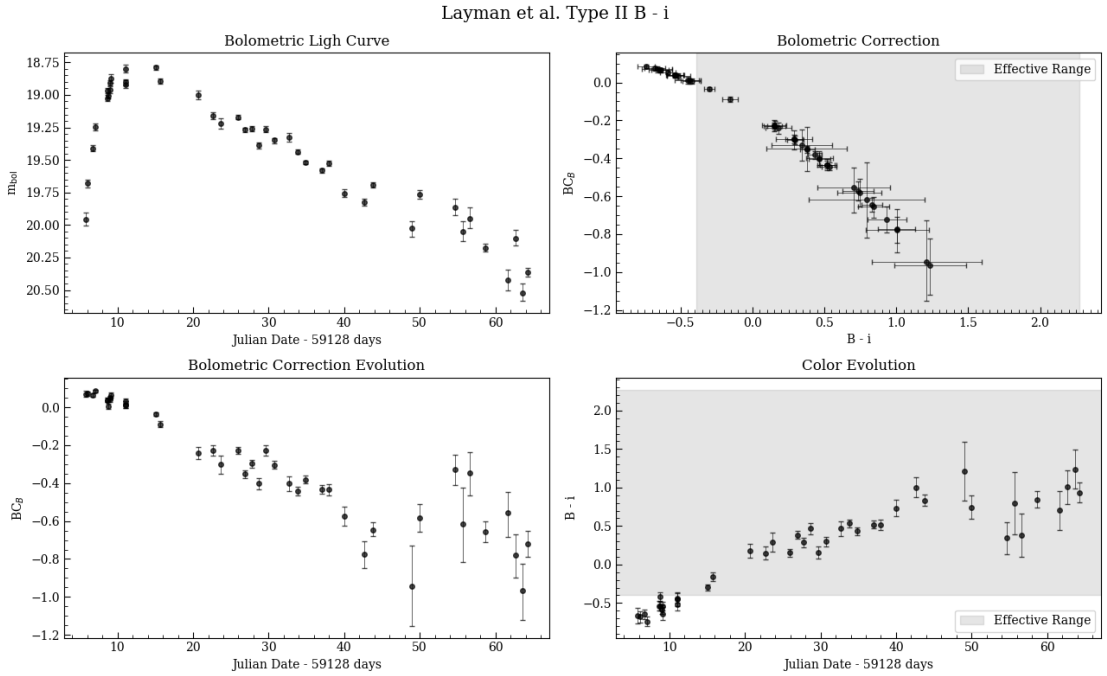

Figure 8: Bolometric corrections from Lyman, Bersier, James, Mazzali, et al. 2016a for (B - i) color as shown in table 3 2^{nd} row.

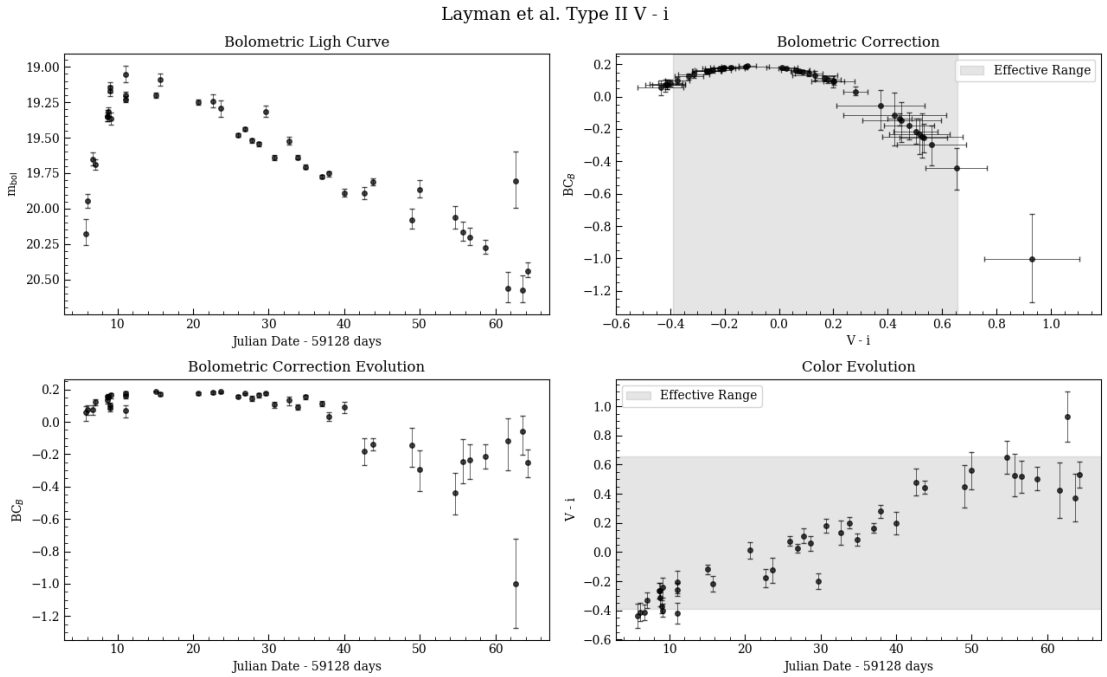

Figure 9: Bolometric corrections from Lyman, Bersier, James, Mazzali, et al. 2016a for (V - i) color as shown in table 3 3^{rd} row.

Carlo simulation on the color evolution curve we can find the corresponding bolometric correction terms for the fitted polynomials. Consequently we can used these terms to compute the bolometric magnitude on the observation dates and use the IQR of sampled population for the error bars in the bolometric magnitude. Using the polynomial with

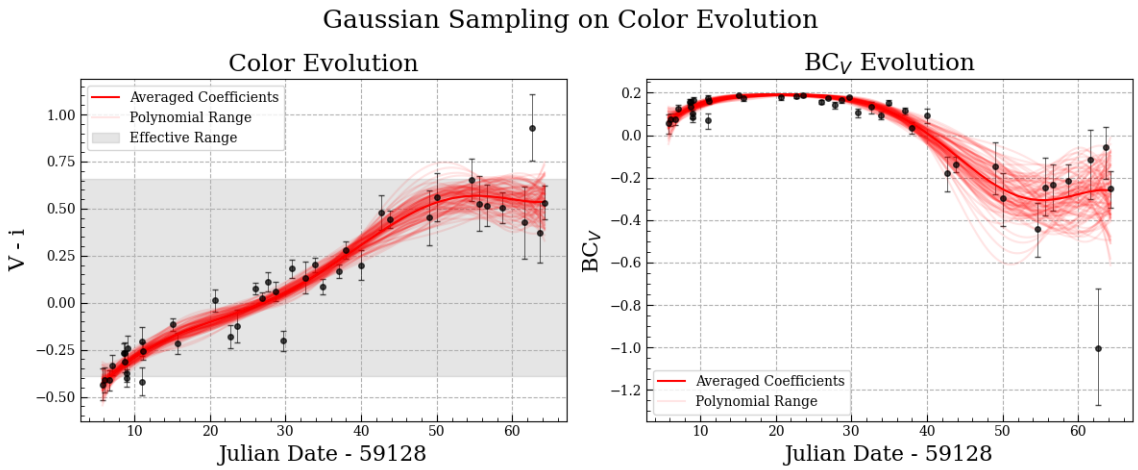

Figure 10: Monte-Carlo Gaussian sampling of color evolution for (V-i) bolometric correction from Lyman, Bersier, James, Mazzali, et al. 2016a. Color data points were fitted to a polynomial of degree 6.

the averaged coefficients as our simulated data and the sampled population at the observation dates we can compute the bolometric magnitudes and their respective uncertainties for this correction.

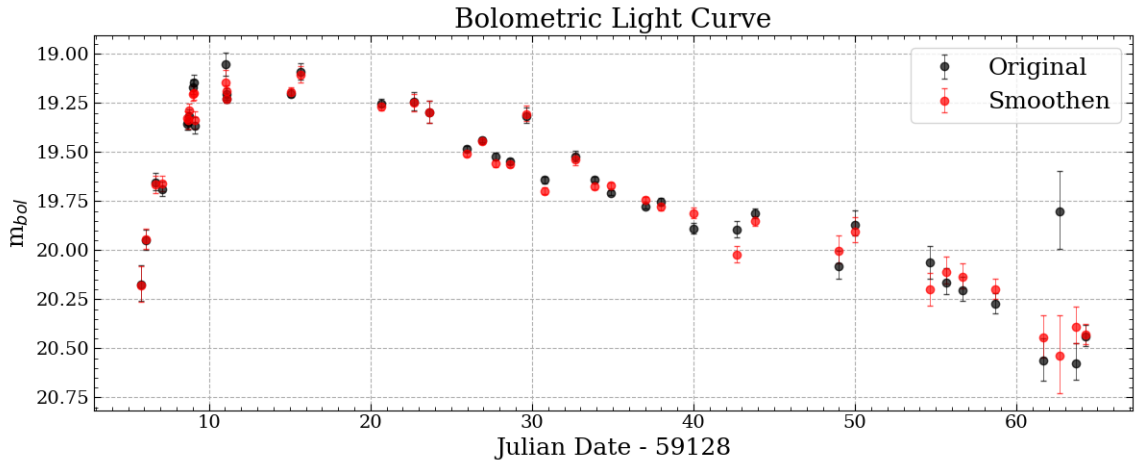

Figure 11: Bolometric light curve for (V - i) correction from Lyman, Bersier, James, Mazzali, et al. 2016a. (Red data) Bolometric magnitudes from Monte-Carlo polynomial fitting and error bars are representative of the 50% confidence interval of the sampled distribution.

3.3. *Final Remarks & Discussion*

Evaluating the 4 bolometric corrections conducted in this paper we believe the corrections that created the best light curves where for the colors (B - i) and (V - i). The main factor that contributed to this decision was the extended color range for these corrections as they covered 69% and 85% of our entire color data respectively, while the (B - V) correction from Martinez et al. 2022 and Lyman, Bersier, and James 2013 only covered 63% and 65% of our total color data points. We can also comment on the Monte-Carlo color fitting in Figure 10 and Figure 11 where we can see how the color that was located outside the effective range was corrected by the polynomial fit simulations. The success of this methods attributed to the nearby data points to the color in question, because these colors are within the expected monotonic trend the polynomials tend to stay within these points rather than diverge to the outlier.

Additionally, from this work we would like to perform spectral analysis on KSP-ZN7090 as this will shed light

on the further spectral classification of the SNe. Which will help us determine if we can use additional bolometric corrections from Lyman, Bersier, and James 2013.

References

Anderson, Joseph P. et al. (Apr. 2014). "Characterizing the V Band Light-Curves of Hydrogen-Rich Type II Supernovae". In: *The Astrophysical Journal* 786.1, p. 67. DOI: 10.1088/0004-637x/786/1/67. URL: https://doi.org/10.1088%2F0004-637x%2F786%2F1%2F67.

Gall, E. E. E. et al. (2015). "A comparative study of Type II-P and II-L supernova rise times as exemplified by the case of LSQ13cuw". In: *A&A* 582, A3. DOI: 10.1051/0004-6361/201525868. URL: https://doi.org/10.1051/0004-6361/201525868.

González-Gaitán, S. et al. (June 2015). "The rise-time of Type II supernovae". In: *Monthly Notices of the Royal Astronomical Society* 451.2, pp. 2212–2229. ISSN: 0035-8711. DOI: 10.1093/mnras/stv1097. eprint: https://academic.oup.com/mnras/article-pdf/451/2/2212/5723895/stv1097.pdf. URL: https://doi.org/10.1093/mnras/stv1097.

Lyman, J. D., D. Bersier, and P. A. James (Dec. 2013). "Bolometric corrections for optical light curves of core-collapse supernovae". In: *Monthly Notices of the Royal Astronomical Society* 437.4, pp. 3848–3862. ISSN: 0035-8711. DOI: 10.1093/mnras/stt2187. eprint: https://academic.oup.com/mnras/article-pdf/437/4/3848/18500482/stt2187.pdf. URL: https://doi.org/10.1093/mnras/stt2187.

Lyman, J. D., D. Bersier, P. A. James, P. A. Mazzali, et al. (Jan. 2016a). "Bolometric light curves and explosion parameters of 38 stripped-envelope core-collapse supernovae". In: *Monthly Notices of the Royal Astronomical Society* 457.1, pp. 328–350. DOI: 10.1093/mnras/stv2983. URL: https://doi.org/10.1093%2Fmnras%2Fstv2983.

– (Jan. 2016b). "Bolometric light curves and explosion parameters of 38 stripped-envelope core-collapse supernovae". In: *Monthly Notices of the Royal Astronomical Society* 457.1, pp. 328–350. ISSN: 0035-8711. DOI: 10.1093/mnras/stv2983. eprint: https://academic.oup.com/mnras/article-pdf/457/1/328/18168167/stv2983.pdf. URL: https://doi.org/10.1093/mnras/stv2983.

Martinez, L. et al. (Apr. 2022). "Type II supernovae from the Carnegie Supernova Project-I". In: *Astronomy &amp Astrophysics* 660, A40. DOI: 10.1051/0004-6361/202142075. URL: https://doi.org/10.1051%2F0004-6361%2F202142075.

Rubin, Adam et al. (Mar. 2016). "TYPE II SUPERNOVA ENERGETICS AND COMPARISON OF LIGHT CURVES TO SHOCK-COOLING MODELS". In: *The Astrophysical Journal* 820.1, p. 33. DOI: 10.3847/0004-637x/820/1/33. URL: https://doi.org/10.3847/0004-637x/820/1/33.

Shappee, B. J. et al. (Dec. 2018). "Seeing Double: ASASSN-18bt Exhibits a Two-component Rise in the Early-time iK2/i Light Curve". In: *The Astrophysical Journal* 870.1, p. 13. DOI: 10.3847/1538-4357/aaec79. URL: https://doi.org/10.3847/1538-4357/aaec79.